Surv Geophys (2009) 30:503–523
DOI 10.1007/s10712-009-9069-z

A Comparison of Strategies for Seismic Interferometry

Roel Snieder · Masatoshi Miyazawa · Evert Slob · Ivan Vasconcelos · Kees Wapenaar

Received: 31 October 2008 / Accepted: 19 March 2009 / Published online: 29 April 2009
© Springer Science+Business Media B.V. 2009

Abstract The extraction of the response from field fluctuations excited by random sources has received considerable attention in a variety of different fields. We present three methods for the extraction of the systems response that are based on cross-correlation, deconvolution, and the solution of an integral equation, respectively. For systems that are invariant for time-reversal the correlation method requires random sources on a bounding surface only, but when time-reversal invariance is broken, for example by attenuation, a volume distribution of sources is needed. For this reason the correlation method is not useful for diffusive or strongly attenuating systems. We provide examples of the three methods and compare their merits and drawbacks. We show that the extracted field may satisfy different boundary conditions than does the physical field. This can be used, for example, to suppress surface-related multiples in exploration seismology, to study the coupling of buildings to the subsurface, and to remove the airwave in controlled source electromagnetics (CSEM).

R. Snieder (✉) · M. Miyazawa · I. Vasconcelos
Center for Wave Phenomena and Department of Geophysics, Colorado School of Mines,
Golden, CO 80401, USA
e-mail: rsnieder@mines.edu

Present Address:
M. Miyazawa
Earthquake Research Institute, University of Tokyo, 1-1-1 Yayoi, Bunkyo-Ku, Tokyo 113-0032, Japan

E. Slob · K. Wapenaar
Department of Geotechnology, Delft University of Technology, 2600 GA Delft, The Netherlands

Present Address:
I. Vasconcelos
ION Geophysical, GXT Imaging Solutions, Egham, Surrey, UK

1 Introduction

The extraction of information from random field fluctuations is a rapidly growing field in physics, acoustics, engineering, and geophysics. The widespread application of this idea has led to a variety of different names used for the method that include Green's function extraction, daylight imaging, the virtual source method, and seismic interferometry. In the exploration seismology community, the name seismic interferometry is now mostly used (Curtis et al. 2006).

The theory for the extraction of the Green's function from field fluctuations has been known in the physics community under the name *fluctuation–dissipation theorem* (Callen and Welton 1951; Weber 1956; Kubo 1966; Rytov et al. 1989; Le Bellac et al. 2004). This theorem states that for a Hamiltonian system in thermodynamic equilibrium the correlation of field fluctuations are related to the impulse response of the system. The name is poorly chosen, because there is, strictly speaking, no dissipation in Hamiltonian systems. Tatarskii (1987) solved this problem by dividing a system that conserves energy into a part one is interested in, and a part that is irrelevant. The energy flow from the first part to the latter part then effectively acts as dissipation. We show that dissipation plays an interesting role in Green's function extraction.

As with so many developments in geophysics, Aki (1957) pioneered the use of near-surface microseismic noise to extract the properties of the near surface. Lobkis and Weaver (2001) gave the field new momentum with their derivation of Green's function extraction based on normal modes. They made two contributions. First, they showed that the Green's function can be extracted assuming that each mode is excited with the same energy, in other words: thermodynamic equilibrium is not essential. This is important, because the field fluctuations in a macroscopic body, such as the Earth, generally are not in thermodynamic equilibrium. Their second contribution is that they showed how useful the Green's function extraction can be in practical applications.

A flurry of applications appeared in different fields that include ultrasound (Weaver and Lobkis 2001, 2003; Malcolm et al. 2004; van Wijk 2006; Larose et al. 2006a), helioseismology (Rickett and Claerbout 1999, 2000), near-surface geophysics (Louie 2001; Chávez-Garcia and Luzón 2005), ocean acoustics (Roux and Fink 2003; Roux et al. 2004; Sabra et al. 2005a), structural engineering (Snieder and Şafak 2006; Snieder et al. 2006a; Thompson and Snieder 2006; Kohler et al. 2007; Sabra et al. 2008), medical diagnostics (Sabra et al. 2007), exploration seismology (Schuster et al. 2004; Bakulin and Calvert 2006; Hornby and Yu 2007; Draganov et al. 2007; Bakulin et al. 2007), crustal seismology (Campillo and Paul 2003; Shapiro and Campillo 2004; Shapiro et al. 2005; Sabra et al. 2005b; Roux et al. 2005), and hazard monitoring (Sabra et al. 2004; Sens-Schönfelder and Wegler 2006; Wegler and Sens-Schönfelder 2007; Brenguier et al. 2008). In most of the applications the system response was extracted by cross-correlating field fluctuations, but the alternative data-processing technique of deconvolution has been applied in some of these studies.

In this work we present and compare different methods to extract information from field fluctuations. In Sect. 2 we present examples of the correlation approach, while Sect. 3 features deconvolution as an alternative. In Sect. 4 we present yet another method to extract the system response, the multidimensional deconvolution method. We compare the merits and drawbacks of these different approaches. In seismology, the attention focused for obvious reasons on wave systems. In most treatments those are assumed not to attenuate. In this work we focus on dissipative systems as well. Examples of such systems include attenuating waves and diffusive fields. Waves in the Earth do attenuate. Diffusive

fields account, for example, for the pore pressure in a reservoir, and for low-frequency electromagnetic waves in conducting media (Griffiths 1999), such as the Earth. In Sect. 5 we present a powerful aspect of interferometry that has not yet been exploited much. The fields obtained from correlation and deconvolution satisfy the same equation as does the original system. These methods are thus guaranteed to give valid states of the field in the real medium. The field extracted with any of the approaches presented in this work, may, however, satisfy different boundary conditions than the real field satisfies. This makes it possible to determine the wave state as if the system satisfied different boundary conditions. We show examples how this can be used.

2 Correlation Approach

We introduce the correlation approach with a data example from Miyazawa et al. (2008) based on noise measurements taken in a borehole over a heavy oil reservoir in Cold Lake, Canada. The locations of the reservoir and the geophones in the borehole are shown in Fig. 1. The heavy oil, at a depth of about 450 m, is almost solid at ambient temperature. In order to mobilize the oil, steam injection in the injection wells in Fig. 1 is used to heat the heavy oil. Pumps and other mechanical equipment at the wellhead create much seismic noise that propagates down the array in the borehole. Representative examples of the

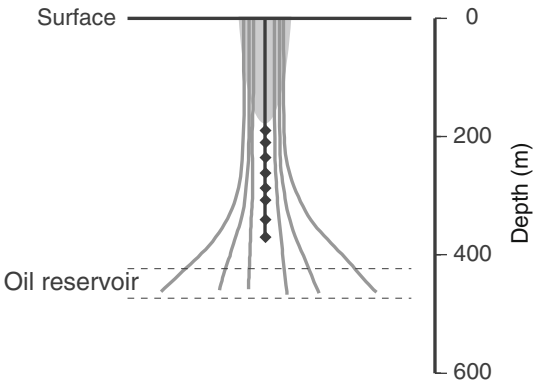

Fig. 1 Geometry of the instrumented borehole with geophones (*diamonds*), injection wells (*grey lines*), and the stationary phase region (*grey shaded area above geophones*)

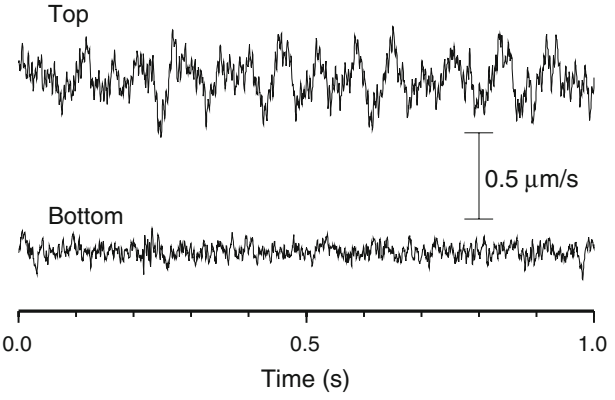

Fig. 2 Example of noise recorded at the top and bottom geophones, respectively

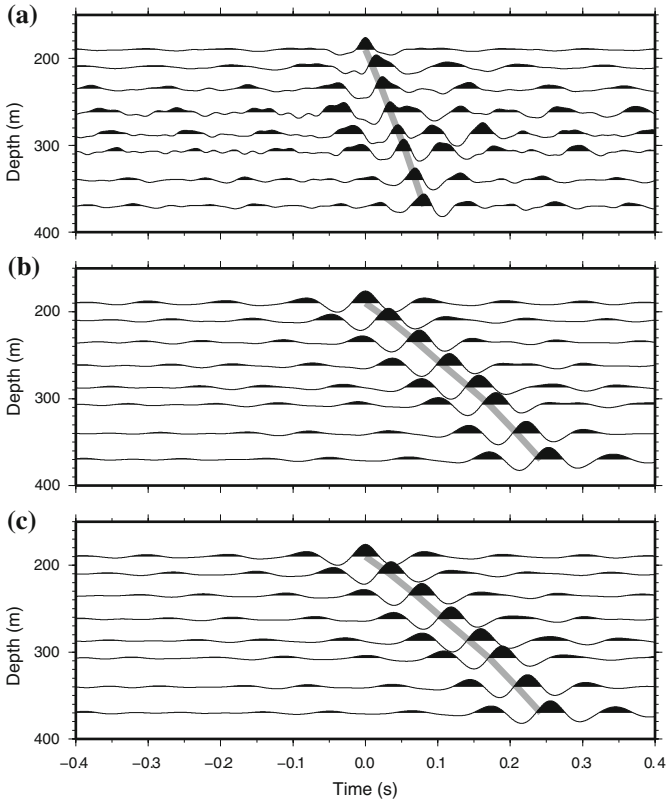

Fig. 3 Cross-correlation between the waveforms at the top sensor and those at other sensors for different components: (**a**) vertical, (**b**) east–west, and (**c**) north–south. *Grey lines* indicate the travel time for P-waves (*panel a*) and S-waves (*panels b and c*). The P and S-wave velocities are known at Cold Lake

recorded noise at the shallowest and deepest sensor in the borehole are shown in Fig. 2. These noise records do not seem to display any order, but there are correlations hidden in the noise; any wave that propagates down the borehole meets the shallowest receiver first and the deeper receiver later.

The underlying order in the recorded noise can be extracted by cross-correlation. Miyazawa et al. (2008) cross correlated for each component 15 s-long records of the noise at the shallowest receiver with the recordings at all other receivers, and averaged the cross correlations measured over a period of 1 month. The result, after bandpass-filtering between 10 and 55 Hz, is shown in Fig. 3 for the three components of the recorded motion. A downward propagating wave is clearly visible in the cross-correlation of the vertical components (panel a), and its arrival time agrees well with the travel time of a downward propagating P-wave. The cross correlation of the signals recorded at the vertical component thus clearly extracts downward propagating P-waves that are hidden in the noise of Fig. 2. The cross correlations of the East–West and North–South components (panels b and c, respectively) show waves that propagate downward with the shear velocity. The cross correlations of the horizontal components successfully extract downward propagating S-waves. By rotating the horizontal components, Miyazawa et al. (2008) were able to measure shear wave splitting based on correlating the noise measurements.

There is a plethora of derivations of the Green's function extraction from cross-correlation starting from the derivation of the fluctuation–dissipation theorem for Hamiltonian systems in thermal equilibrium (Callen and Welton 1951; Weber 1956). Derivations based on normal modes are particularly elegant (Tatarskii 1987; Lobkis and Weaver 2001). Only closed systems have, in general, normal modes. Alternative derivations, also valid for open systems of acoustic waves, have been developed using time-reversal invariance (Derode et al. 2003a, b; Bakulin and Calvert 2004), representation theorems (Wapenaar et al. 2005; Wapenaar and Fokkema 2006), and the summation of random incident plane waves (Weaver and Lobkis 2005). The derivation based on representation theorems has been extended to elastic waves (Wapenaar 2004).

For the Fourier convention $f(t) = \int F(\omega)\ \exp(-i\omega t)d\omega$, where ω is the angular frequency, the extraction of the frequency domain Green's function for acoustic waves is formulated mathematically as (Snieder et al. 2007a)

$$G(\mathbf{r}_A, \mathbf{r}_B) - G^*(\mathbf{r}_A, \mathbf{r}_B) = 2i\omega \oint_{\partial V} \frac{1}{\rho(\mathbf{r})c(\mathbf{r})} G(\mathbf{r}_A, \mathbf{r}) G^*(\mathbf{r}_B, \mathbf{r}) dS. \tag{1}$$

In this expression $G(\mathbf{r}_A, \mathbf{r}_B)$ is the Green's function that accounts for wave propagation from $\mathbf{r}_B$ to $\mathbf{r}_A$, ρ the mass density, c the wave velocity, and the asterisk denotes complex conjugation. The integration is over a closed surface ∂V that encloses receivers at $\mathbf{r}_B$ and $\mathbf{r}_A$. Since a radiation boundary condition is used in this derivation (Wapenaar et al. 2005), the closed surface must be sufficiently far from the receivers. Expression (1) and all other expressions in this work are valid in the frequency domain. For brevity the frequency-dependence is omitted throughout this work.

We first establish the connection with random pressure sources q at the boundary ∂V that excite field fluctuations. Suppose that these sources are spatially uncorrelated and satisfy

$$\langle q(\mathbf{r}_1) q^*(\mathbf{r}_2) \rangle = \frac{|S(\omega)|^2}{\rho(\mathbf{r}_1)c(\mathbf{r}_1)} \delta(\mathbf{r}_1 - \mathbf{r}_2) \tag{2}$$

where $|S(\omega)|^2$ is the power spectrum of the noise and $\langle \cdots \rangle$ denotes an ensemble average. In practice this ensemble average is replaced by a time average (Larose et al. 2006b). The integral in expression (1) can be written as $\oint\oint (\rho(\mathbf{r}_1)c(\mathbf{r}_1))^{-1} G(\mathbf{r}_A, \mathbf{r}_1)\delta(\mathbf{r}_1 - \mathbf{r}_2)$ $G^*(\mathbf{r}_B, \mathbf{r}_2) dS_1 dS_2$, together with Eq. 2 this gives

$$G(\mathbf{r}_A, \mathbf{r}_B) - G^*(\mathbf{r}_A, \mathbf{r}_B) = \frac{2i\omega}{|S(\omega)|^2} \langle p(\mathbf{r}_A) p^*(\mathbf{r}_B) \rangle, \tag{3}$$

where $p(\mathbf{r}_0) = \oint G(\mathbf{r}_0, \mathbf{r}) q(\mathbf{r}) dS$ are the field fluctuations excited by the random sources on the bounding surface. When sources are present only on part of the bounding surface, the correlation may lead to unphysical arrivals (Snieder et al. 2006b, 2008; Mehta et al. 2008a).

Since complex conjugation in the frequency domain corresponds to time-reversal in the time domain, the left hand side corresponds, in the time domain, to $G(\mathbf{r}_A, \mathbf{r}_B, t) - G(\mathbf{r}_A, \mathbf{r}_B, -t)$, i.e. the superposition of the causal and time-reversed causal Green's functions. The product $p(\mathbf{r}_A)\ p^*(\mathbf{r}_B)$ in the frequency domain corresponds to correlation in the time domain. Expression (3) thus relates the average field fluctuations to the Green's function. Note the presence of the power spectrum $|S(\omega)|^2$ in this expression. Even though one does not need to know the noise spectrum $S(\omega)$, the power spectrum of the excitation must be

known. Also note that for the employed normalization the excitation in expression (2) must be inversely proportional to the acoustic impedance ρc at each source location. For acoustic waves, $p/\rho c$ is proportional to the particle velocity v, hence $|p|^2/\rho c$ is proportional to p^*v, which is the power flux (Morse and Ingard 1968). This means that the power flux flowing from every point on the surface must be constant if the Green's function is to be extracted. This is the property of *equipartitioning* of the energy flow which is shown to be necessary property for Green's function extraction from noise (Lobkis and Weaver 2001; Snieder et al. 2007a).

Let's consider the waves extracted from noise in Fig. 3 again. According to expression (3), cross-correlation of the noise should give both the causal and a-causal Green's function, while Fig. 3 shows waves for positive times only. The reason is that most noise is generated at the top of the borehole and results in waves that are radiated downward. The heavy oil below the array is strongly attenuating, and generates almost no reflected waves that travel upward. Since there is little energy propagating upward along the array, the cross-correlation does not extract these waves. The requirement of equipartitioning is clearly not justified, but the downward propagating P and S-waves can be extracted successfully.

According to expression (1), the noise sources must be placed all over the bounding surface. Yet only sources that launch waves that physically propagate between the receivers give a contribution to the Green's function extraction. In Fig. 1 those source locations are marked with grey shading. Mathematically the importance of these source locations is formulated as follows. The integrand in expression (1) is oscillatory. One can show that the dominant contribution to the integral comes from the *stationary source positions* where the integrand to first order does not vary with the source location (Snieder 2004; Snieder et al. 2006b). The contribution from sources at other locations integrates to zero (Wapenaar et al. 2005; Snieder et al. 2008; Mehta et al. 2008a), provided that the source density is sufficiently high to sample the oscillatory contribution to the integral adequately.

Since noise sources in practice have a strength that varies with time, it is useful to normalize the noise before cross-correlation. Such normalization also helps suppress brief noise burst that may dominate the cross-correlation. The simplest form of such normalization is to replace the recorded noise by its sign bit (Larose et al. 2004), but a variety of other normalization schemes have been developed (Bensen et al. 2007).

The extraction of the Green's function is not limited to loss-less acoustic waves. The theory has been generalized to elastic waves (Wapenaar 2004). The principle can also be applied to the diffusion equation, the counterpart of expression (1) for solutions of the diffusion equation $\partial p/\partial t = \nabla \cdot (D\nabla p)$ is given by Snieder (2006)

$$G(\mathbf{r}_A, \mathbf{r}_B) - G^*(\mathbf{r}_A, \mathbf{r}_B) = 2i\omega \int_V G(\mathbf{r}_A, \mathbf{r}) G^*(\mathbf{r}_B, \mathbf{r}) dV. \tag{4}$$

Apart from the absence of the impedance $1/\rho c$ in the integrand, the main difference with expression (1) is that the surface integral is replaced by a volume integral. That means that the extraction of the Green's function for diffusive fields, such as pore-pressure or electromagnetic fields in a conductive medium, requires that the sources of the field fluctuations are distributed throughout the volume. This requirement has serious consequences, because in practical situation the sources of the field fluctuations may not be present throughout the volume. For attenuating acoustic waves, sources proportional to the local attenuation rate must be present both on the bounding surface ∂V as well as within the

volume (Snieder 2007), but in practice the volume sources need not be strong when the attenuation is weak (Slob et al. 2007). The Green's function extraction by cross-correlation holds for general scalar and vector systems (Wapenaar et al. 2006; Snieder et al. 2007a; Weaver 2008).

3 Deconvolution Approach

Correlation and deconvolution are closely related processes. Early work on the deconvolution approach was applied to wave motion recorded in boreholes (Trampert et al. 1993), this has been extended later to downhole receiver functions (Mehta et al. 2007a). Here we describe applications to problems with a more general geometry. Let us assume, for the moment, that a field is excited with a source at location $\mathbf{r}$ with frequency spectrum $S(\omega)$. The field at locations $\mathbf{r}_A$ and $\mathbf{r}_B$, respectively is given by $p(\mathbf{r}_{A,B}) = G(\mathbf{r}_{A,B}, \mathbf{r})S(\omega)$. The deconvolution of these fields is, in the frequency domain, given by

$$V_{AB} = \frac{p(\mathbf{r}_A)}{p(\mathbf{r}_B)} = \frac{G(\mathbf{r}_A, \mathbf{r})}{G(\mathbf{r}_B, \mathbf{r})} = \frac{G(\mathbf{r}_A, \mathbf{r})G^*(\mathbf{r}_B, \mathbf{r})}{|G(\mathbf{r}_B, \mathbf{r})|^2}. \tag{5}$$

According to the second identity, the deconvolution does not depend on the excitation at all. In the correlation approach, as described in the previous section, the power spectrum of the excitation must be known. In the deconvolution approach it is not necessary to know anything about the excitation.

The numerator in the last term of Eq. 5 describes the correlation of the Green's function that is similar to the integrand of expression (1). This suggest that deconvolution and correlation give virtually the same results. This would indeed be the case when the power spectrum $|G(\mathbf{r}_B, \mathbf{r})|^2$ in the denominator would be a smooth function of frequency. But this is not necessarily the case, especially for the important application where the Green's function consists of the superposition of interfering waves. The resulting notches in the power spectrum may make the power spectrum of the Green's function rapidly fluctuating with frequency. In this case one cannot expect that the deconvolution resembles the correlation.

The property that the deconvolution does not depend on the source spectrum is desirable, but this property comes at a price. Consider the special case where the points $\mathbf{r}_A$ and $\mathbf{r}_B$ coincide. In that case the deconvolution in Eq. 5 reduces to $V_{AA}(\omega) = 1$, which, in the time domain, corresponds to

$$V_{AA}(t) = \delta(t). \tag{6}$$

This means that the field obtained by deconvolution vanishes for nonzero time when the receivers coincide. Physically this means that the deconvolved fields satisfy a *clamped boundary condition* (Vasconcelos and Snieder 2008a) at one of the receivers. This tells us that deconvolution does not give the true Green's function, unless that Green's function also happens to satisfy a clamped boundary condition at that receiver. In that case, the field fluctuations would vanish as well at that receiver, and there would be nothing to record.

It is, however, not needed to deal with the clamped boundary condition when a perturbation approach is used. Suppose that the medium can be divided in a reference medium with field p_0 and Green's function G_0, and a perturbation with associated perturbations p_S and G_S in the field and Green's function, respectively. The reference medium could be a smoothly varying medium, and the perturbation could be rough medium fluctuations that

generate reflected waves, but alternatively the reference medium could account for the subsurface before a time-lapse perturbation, and the perturbation could be the time-lapse change. The latter approach is natural in monitoring applications (Snieder et al. 2007b).

Suppose one can separate for each source at location $\mathbf{r}$ the field into the field perturbation and the unperturbed field, and that one deconvolves those fields:

$$V'_{AB} = \frac{p_S(\mathbf{r}_A)}{p_0(\mathbf{r}_B)} = \frac{G_S(\mathbf{r}_A,\mathbf{r})}{G_0(\mathbf{r}_B,\mathbf{r})} = \frac{G_S(\mathbf{r}_A,\mathbf{r})G_0^*(\mathbf{r}_B,\mathbf{r})}{|G_0(\mathbf{r}_B,\mathbf{r})|^2}. \tag{7}$$

Integration over all sources gives

$$\int_{\partial V} V'_{AB} dS = \int_{\partial V} \frac{G_S(\mathbf{r}_A,\mathbf{r})G_0^*(\mathbf{r}_B,\mathbf{r})}{|G_0(\mathbf{r}_B,\mathbf{r})|^2} dS. \tag{8}$$

When the reference medium is smooth, G_0 does not consist of many interfering waves and usually is a smooth function of frequency. The numerator in expression gives the correlation between wavefield perturbations at $\mathbf{r}_A$ and unperturbed waves at $\mathbf{r}_B$. When the source is at such a location that it launches direct waves to $\mathbf{r}_B$ that are then reflected by the medium perturbation to propagate to $\mathbf{r}_A$, one retrieves the perturbed waves that propagate from $\mathbf{r}_B$ to $\mathbf{r}_A$ (Vasconcelos and Snieder 2008a). It suffices to sum over a range or sources near the stationary phase region for these arrivals. In practice one does not know the precise location and extent of the stationary phase regions, and one employs sources over a larger region that can be assumed to include the stationary phase zones.

In this approach one needs to separate the unperturbed field from the field perturbations. For waves this can sometimes be done using a time gate that separates the direct waves from reflected waves. This does, however, not work when the excitation has a long duration in the time domain. In that case the direction of wave propagation may be used to carry out this separation. For example, the direct wave may propagate downward, while the reflected waves travel upward. For acoustic waves, such up-down separation can be carried out with dual-sensor summation (Robinson 1999) when both the pressure and displacement are measured. When an array of sensors is available, frequency-wavenumber filtering can be used to separate the waves propagating in different directions along the array. With a borehole array internal multiples can be used to illuminate a target above the downhole array to provide unique bottom-side images of, for example, a salt dome (Vasconcelos et al. 2008a). In that application beam-steering was used to separate the unperturbed and perturbed waves and illuminate desired target regions.

We illustrate deconvolution with a synthetic example (Vasconcelos and Snieder 2008b) in which drill bit noise is used as a seismic source. In drill bit seismology the vibrations in the drill bit usually are recorded in order to provide the excitation of elastic waves by the drill bit (Rector and Marion 1991; Poletto and Miranda 2004). For a long drill stem the vibrations reverberating in the drill stem make it difficult to retrieve the desired excitation of waves at the drill bit from vibrations recorded at the top of the drill stem, and more complicated dual sensor measurements have been used to reduce those reverberations (Poletto et al. 2004). In the approach with deconvolution interferometry there is, however, no need to record the vibrations in the drill stem.

As shown in the left panel of Fig. 4 a drill bit under the salt dome radiates noise, this noise is detected on an array of geophones in a borehole. Each geophone acts, in turn, as the reference receiver for deconvolution interferometry. In practice this is realized by deconvolving the motion at every geophone with the motion at the employed reference receiver.

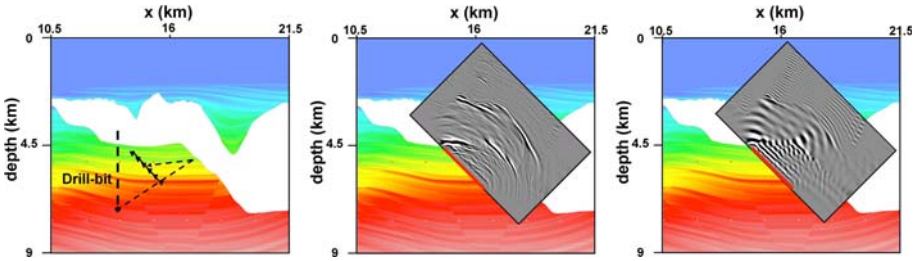

Fig. 4 *Left panel*: the sigsbee model with a salt body shown in *white*. The hypothetical location of a drill bit and receivers (*triangles*) in a borhole are shown. *Middle panel*: the image obtained from deconvolution interferometry. *Right panel*: the image obtained from correlation interferometry

This gives the underside reflections of the salt body that propagate from the target receiver to the other receivers of the array. Beam-stearing can be used to direct the waves towards the target that one aims to image (Vasconcelos and Snieder 2008b; Vasconcelos et al. 2008a). According to expression (5) the deconvolved waves do not depend on the unknown source signal, hence there is no need to record the vibrations of the drill bit in this approach.

The reflected waves thus obtained can be used to image the salt body as if physical sources were placed in the instrumented well. The resulting image is shown in the middle panel of Fig. 4. The bottom and top of the salt body are clearly visible in this image. Only parts of the salt body are imaged; this is due to the limited aperture of the borehole array. Vasconcelos and Snieder (2008b) and Vasconcelos et al. (2008b) used imaging based on deconvolution interferometry applied to drill bit noise recorded in the pilot hole of the San Andreas Fault Observatory at Depth (SAFOD) as the main hole was drilled, to carry out broadside imaging of the San Andreas fault.

The right panel of Fig. 4 shows what happens if the image is obtained by using correlation instead of deconvolution and using the waves thus obtained to create an image. The image thus obtained is dominated by strong reverberations. According to Eq. 3 one must divide by the power spectrum in the correlation approach to retrieve the Green's function. This division was not carried out in the data processing leading to the image in the right panel on Fig. 4 because in practice the power spectrum of the drill bit noise often is poorly known. As a result, the waveforms obtained by cross-correlation are the Green's function convolved with the autocorrelation of the drill bit noise. Since this noise is narrow-band, this autocorrelation is oscillatory, and the resulting image therefore also shows pronounced ringing.

4 Multidimensional Deconvolution Approach

This approach can be seen as a generalization of the deconvolution method described in the previous section. The central idea (Wapenaar et al. 2000; Amundsen 2001) is sketched in Fig. 5. Suppose sensors measure the field on an acquisition surface indicated with the solid line. Let's assume that the total field at every location can be decomposed in a downgoing field D and upgoing field U. For acoustic waves this decomposition can be carried out by combining pressure and particle velocity using dual sensor summation (Robinson 1999; Pharez et al. 2008), or alternatively by towing streamers in marine seismology using the over-under configuration (Hill et al. 2006; Moldoveanu et al. 2007). For electromagnetic fields the up-down separation can be achieved by making suitable combinations of electric

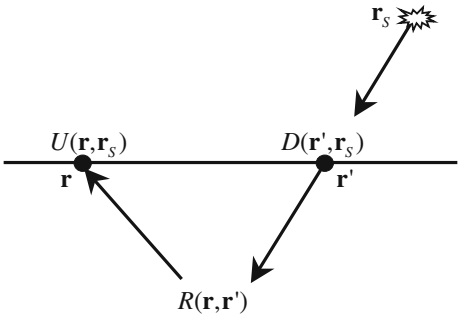

Fig. 5 The downgoing field $D(\mathbf{r}', \mathbf{r}_S)$ at $\mathbf{r}'$, the upgoing field $U(\mathbf{r}, \mathbf{r}_S)$ at $\mathbf{r}$ and the reflectivity operator $R(\mathbf{r}, \mathbf{r}')$ that relates these fields. A source at $\mathbf{r}_S$ excites these fields. The fields do not necessarily propagate along straight lines and the source can be extended

and magnetic fields (Amundsen et al. 2006). The downgoing field at location $\mathbf{r}'$ is related to the upgoing field at location $\mathbf{r}$ by a reflectivity operator $R(\mathbf{r}, \mathbf{r}')$. This reflectivity operator is not the Green's function, since it does not give the response to a unit source at $\mathbf{r}'$, but instead relates the upgoing field at $\mathbf{r}$ generated by a unit downgoing field at $\mathbf{r}'$. This operator can be used, though, for imaging the region under the acquisition surface.

In Fig. 5 the upgoing and downgoing fields are indicated by straight lines, but that does not imply that the fields propagate in a homogeneous medium. In fact, the fields propagate through the real subsurface, which can be arbitrarily heterogeneous. Figure 5 depicts a point source at location $\mathbf{r}_S$, but in reality the source may have a finite extent. We simply use the coordinate $\mathbf{r}_S$ to label different sources. The source signal need not be known in the following. In the frequency domain the upgoing field is formed by the superposition of the downgoing field at all locations multiplied with the reflectivity operator

$$U(\mathbf{r}, \mathbf{r}_S) = \int R(\mathbf{r}, \mathbf{r}')D(\mathbf{r}', \mathbf{r}_S)dS', \tag{9}$$

where the integration $\int \cdots dS'$ is over the locations $\mathbf{r}'$ in the acquisition surface.

When the upgoing and downgoing fields are known, Eq. 9 is an integral equation for the reflectivity $R(\mathbf{r}, \mathbf{r}')$. For a single source the solution of this equation is ill-posed. Physically this can be understood as follows. Suppose one has just one source at location $\mathbf{r}_S$, then it makes sense that one can not retrieve the reflectivity operator $R(\mathbf{r}, \mathbf{r}')$ for all locations $\mathbf{r}$ and $\mathbf{r}'$, especially when the source is not at a favorable location as it is in Fig. 5. When there are, however, many sources at different locations $\mathbf{r}_S$, one can use the combined set of equations (9) for all sources to solve for the reflectivity operator. The number of sources that are needed in practice for a stable reconstruction of the reflectivity operator depends on the frequency of the involved fields, the complexity of those fields, and on the location of those sources.

The connection with the deconvolution method of the previous section follows by assuming that downgoing fields are only present at one fixed location $\mathbf{r}'$ and that the downgoing field corresponds to the unperturbed field while the upgoing field is the field perturbation. In that case $U(\mathbf{r}, \mathbf{r}_S) = R(\mathbf{r}, \mathbf{r}')\ D(\mathbf{r}', \mathbf{r}_S)$, and the reflectivity follows by deconvolving upgoing and downgoing fields: $R(\mathbf{r}, \mathbf{r}') = U(\mathbf{r}, \mathbf{r}_S)/D(\mathbf{r}', \mathbf{r}_S)$. The deconvolution method of the previous section can thus be seen as an approximation to the multidimensional deconvolution method.

A major advantage of the multidimensional deconvolution approach is that the retrieved reflectivity depends neither on the medium parameters above the acquisition surface, nor on the possible presence of a free-surface above the acquisition surface. The multidimensional deconvolution method is akin to *Noah's deconvolution* proposed by Riley and

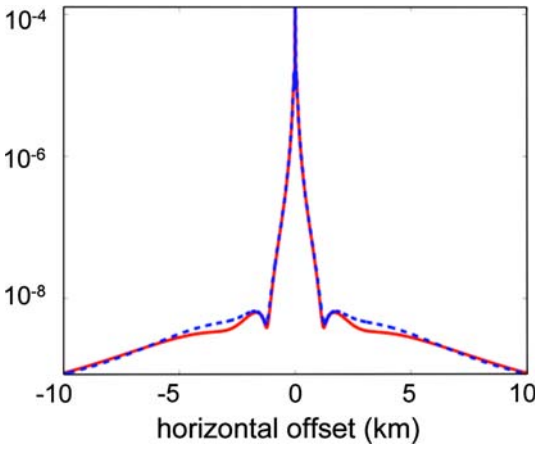

Fig. 6 Electric field for the model without reservoir (*dashed curve*) and the model with a reservoir (*solid curve*)

Claerbout (1976), in which the ocean with a free surface is replaced by an unbounded water layer above the acquisition surface. Because of this replacement the retrieved estimate of the reflectivity is not influenced by the reflections off the free surface above the acquisition plane.

Note that the multidimensional deconvolution method can be applied to any kind of field. We show an example of electromagnetic fields that propagate in the Earth's subsurface. Because of the electrical conductivity and employed frequency (0.25 Hz), such fields are of a diffusive nature, except in the air where the field propagates as a wave. This application is of particular interest because in marine applications the propagation of electromagnetic fields through a shallow water layer and the air above is a known complication (Um and Alumbaugh 2007).

The synthetic example of Figs. 6 and 7 is for the special case of a layered two dimensional earth model. Figure 6 shows the electric field for two models, one with a hydrocarbon reservoir at a depth of 1150 m and one without the reservoir. The horizontal offset in Fig. 6 is measured relative to the source location, the source was placed 25 m above the water bottom where the sensors were assumed to be located. In both cases the aquisition surface is covered by a water layer with a thickness of 500 m, details can be found in Wapenaar et al. (2008). Note that the difference in the electric fields for the model with and without the reservoir is extremely small, and that this difference can only be seen in field values that are about four orders of magnitude smaller than the fields measured near the source. This means that in order to detect the presence of the reservoir one needs measurements with a large dynamic range and low noise level.

Figure 7 shows the reflectivity R for the electric field obtained by numerically solving integral equation (9). Note that the response with and without the reservoir now differs for field values that are only one order of magnitude smaller than the peak response. This means that the reflectivity is much more sensitive to the presence or absence of the reservoir than is the total electric field. Physically, the reason for this is that the total electric field is dominated by the downgoing field, whereas the presence of the reservoir is mostly imprinted on the upgoing field. The up/down separation thus enhances the sensitivity to the presence of the reservoir. In addition, the total electric field in Fig. 6 is influenced by the air wave, and hence depends on the water depth. In contrast, the reflectivity in Fig. 7 is independent on the overburden, and hence it is not influenced by the airwave. Because of its independence of the overburden, the reflectivity is the same

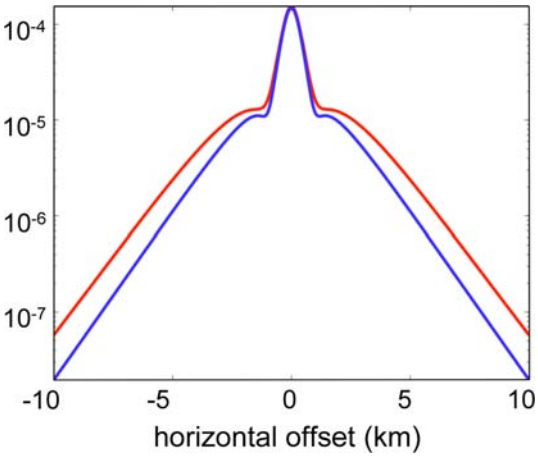

Fig. 7 Reflectivity R for the model without reservoir (*bottom curve*) and the model with a reservoir (*top curve*)

regardless of the water depth. This makes the multidimensional deconvolution approach especially attractive for applications of controlled source electromagnetics in shallow water, where the airwave is of particular concern.

5 Changing the Boundary Condition

It is not widely known that in the Green's function extraction one can alter the boundary conditions of the system. For the correlation and deconvolution approaches the extracted response satisfies the same field equation as does the physical system (Snieder et al. 2006a). The boundary condition of the extracted responses can differ, however, from the original physical fields. For the multidimensional deconvolution the imprint of the overburden above the acquisition surface is completely removed. This means in seismic applications that multiples reflected from the free surface are eliminated (Wapenaar et al. 2000; Amundsen 2001), while for electromagnetic waves the contaminating of the air wave is removed (Wapenaar et al. 2008). The change in the surface boundary condition also forms the basis of other methods for the suppression of surface-related multiples in seismology (Riley and Claerbout 1976; Kennett 1979; Verschuur et al. 1992; van Borselen et al. 1996; Weglein et al. 1998).

We illustrate the freedom to change the boundary conditions in seismic interferometry with the response of the Millikan library at Caltech extracted from recorded vibrations of the building after an earthquake (Snieder and Şafak 2006). This building is shown in the left panel of Fig. 8 and the location of accelerometers in the basement and the ten floors is marked with solid circles. The north–south component of the acceleration after the Yorba Lina earthquake is shown in the right panel. The motion increases with height in the building because of the increased sway of the building with height.

The response extracted by deconvolving the motion at every floor with the motion in the basement is shown in Fig. 9. As discussed in Sect. 3 the extracted response now satisfies a clamped boundary condition in the basement, and indeed, in Fig. 9 the motion is a bandpass-filtered delta function in the basement. For nonzero times, the extracted motion in the basement vanishes. This is, of course, not the case for the real building. In fact, one can see in the bottom trace of the original data in Fig. 8 that the building is being shaken at its base throughout the arrival of the body wave coda and the surface waves that excite the

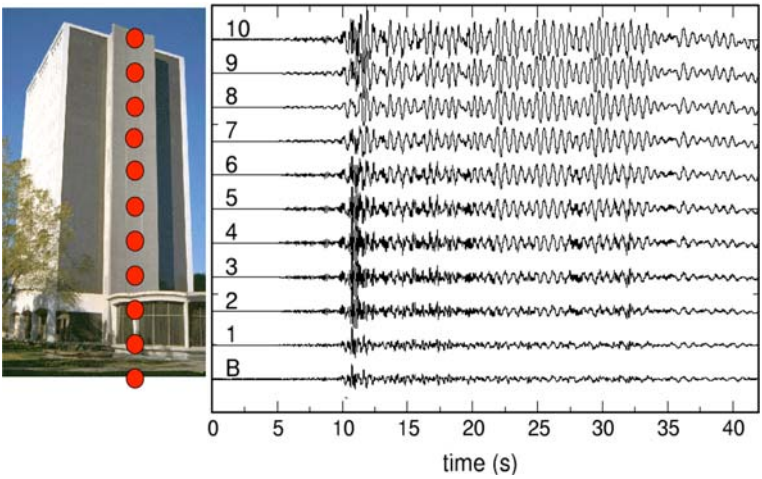

Fig. 8 *Left panel*: the Millikan library at Caltech with the location of accelerometers. *Right panel*: north–south component of acceleration after the Yorba Linda earthquake of 03 Sep 2002 (ML = 4.8, Time: 02:08:51 PDT, 33.917 N 117.776 W Depth 3.9 km). The traces are labeled with the floor number (*B* indicates basement)

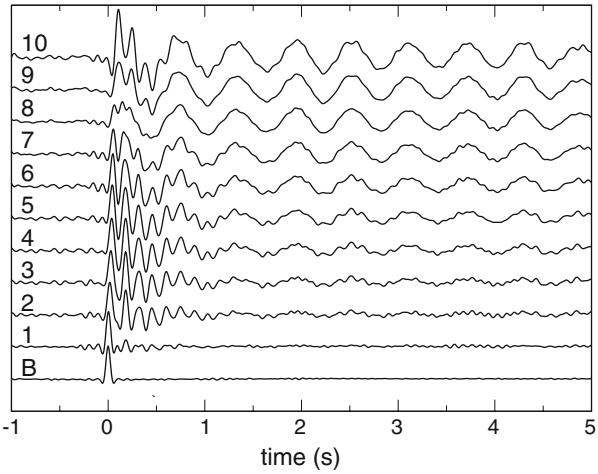

Fig. 9 Waveforms of Fig. 8 after deconvolution with the motion in the basement

building. In contrast, the extracted response in Fig. 9 is for a fictitious building whose base is excited by a bandpass filtered delta pulse and then remains fixed. Such a fictitious building has reflection coefficient $R = -1$ at the base, which precludes the transmission of energy from the subsurface into the building!

As another example we present in Fig. 10 the motion of the Millikan library after deconvolution with the motion at the top floor. Now the motion at the top floor is collapsed into a bandpass-filtered delta function. Note that this response is a-causal, but it still is a valid wave state of the building that consists of one upgoing wave that is reflected by the top of the building into a downgoing wave. Note that this downgoing wave is not reflected at the base of the building, this wave state thus corresponds to a fictitious building that has reflection coefficient $R = 0$ at its base. Physically, the reflection coefficient vanishes for

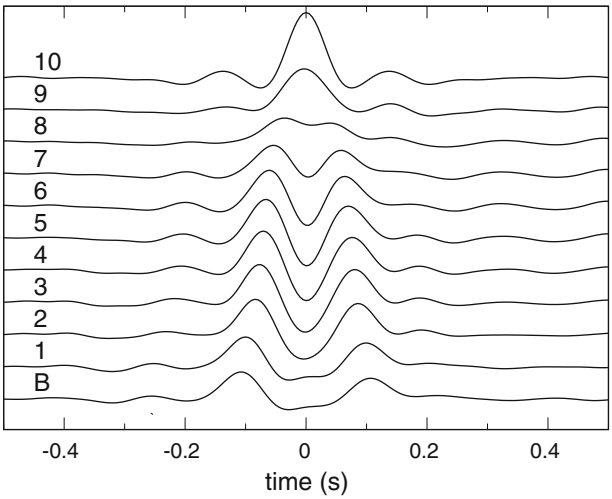

Fig. 10 Waveforms of Fig. 8 after deconvolution with the motion at the top floor

this wave state because now the the deconvolved motion at the top floor is a bandpass-filtered delta function, hence the deconvolved motion at the top vanishes for nonzero time. Because of the absence of significant internal reflections in the building, see Fig. 10, any wave reflected upward at the base of the building would cause a nonzero displacement at the top for $t > 0$. Since the deconvolution precludes such motion, the base of the building must be reflection-less for this wave state. This would not be the case if the building would generate significant internal reflections.

The examples of Figs. 9 and 10 show that from the same data one can retrieve wave-states that satisfy different boundary conditions. The real building has neither reflection coefficient $R = -1$ nor $R = 0$. In the first case, energy would not be able to be transmitted into the building, while the latter case precludes the resonance that is clearly visible in Fig. 8, because all wave energy is radiated downward at the base. Examples of wave-states of the building that have reflection coefficient $R = 0$, but that are either purely causal or a-causal can be found in Snieder et al. (2006a). Note that the extracted response in the Figs. 9 and 10 is solely based on processing of the recorded motion in Fig. 8. It does not involve numerical modeling of the building and the mechanical properties of the building need not be known.

In marine seismology the idea to change the boundary condition is of particular importance because reflections from the free surface, called multiples, often are stronger than the reflections from the reservoir one is interested in. Mehta et al. (2007b, 2008b) applied seismic interferometry to ocean-bottom data recorded over the Mars field in the Gulf of Mexico. By applying up/down separation by dual sensor summation and time-gating of the direct wave they extracted virtual shot records in which the waves reflected off the ocean's free surface are almost perfectly eliminated.

6 Applications to Crustal Seismology

In global and crustal seismology, interferometry has been used extensively. The cross-correlation of noise recordings gives estimates of the Green's function that are dominated

by the fundamental mode surface wave. This has been used exploited to carry out surface wave tomography (Shapiro and Campillo 2004; Shapiro et al. 2005; Sabra et al. 2005b; Ritzwoller 2009). Interferometry allows for the extraction of the surface waves that propagate between any pair of sensors in a seismic network. The illumination thus obtained is vastly superior to that obtained using earthquakes as a seismic source. The application to US Array, a dense seismic network that covers the United States, is particularly promising for high-resolution imaging on a continental scale (Yang and Ritzwoller 2008).

Although some studies successfully extract body waves from cross-correlation of noise (Roux et al. 2005; Sabra et al. 2004), the body waves are, in general, under-represented. This is due to inadequacies in the distribution of sources that excite the noise. In some cases, exotic natural sources such as hurricance Katrina (Gerstoft et al. 2006) and non-volcanic tremor (Chaput and Bostock 2007) have been useful for extracting body waves. Equation 1 states that for acoustic waves the field fluctuations must be excited with equal strength over a closed surface surrounding the receivers. A similar property holds for elastic waves (Wapenaar 2004). According to expression (3), cross-correlation of field fluctuations gives a superposition of the Green's function and the time-reversed Green's function that have equal strength. In seismological applications, the causal surface wave extracted by cross correlation and its time-reversed counterpart often are of different strength. Paul et al. (2005) show, for example, that for an array in Alaska the strongest surface wave propagates away from the ocean. In fact, it has been shown using beam-forming that most seismic noise is generated by storms on the ocean (Stehly et al. 2006). This is consistent with theory and observations of the generation of seismic noise (Gutenberg 1947; Longuet-Higgins 1950; Webb 1998). Because of the spatial distribution of the oceans and the localized presence of depressions that generate ocean waves, the noise distribution is far from uniform. To a certain extent such limitation in the distribution of the sources of field fluctuations can be remedied by cross-correlating the coda waves that were obtained themselves by cross-correlation (Stehly et al. 2008). Since the coda waves propagate in more directions than do the direct surface waves, this procedure provides a better sampling of the field fluctuations.

The continuous presence of noise makes interferometry a useful tool for monitoring since one can extract a Green's function in a quasi-continuous fashion. This has been used to monitor Merapi volcano (Sens-Schönfelder and Wegler 2006). Unfortunately, since the extraced Green's function was dominated in that study by waves propagating in the near-surface, the extracted Green's function correlated better with precipitation than with the volcanic eruption. Interferometry has successfully been used to monitor changes in the seismic velocity associated with earthquakes (Wegler and Sens-Schönfelder 2007; Brenguier et al. 2008). Deconvolution interferometry applied to borehole data recorded during an earthquake has made it possible to detect the weakening of the near-surface layer due to the shaking (Sawazaki et al. 2009).

7 Discussion

We present three methods for combining field fluctuations with the goal to extract the system's response from these fluctuations. As shown in the examples of Sect. 5 it makes a big difference which data are combined, and how this is done. This may leave the reader in a confused state what the merits and drawbacks of the various approaches are. We summarize these in Table 1.

The correlation method is exact in the sense that formal proofs exist that it gives the Green's function provided adequate sources are present to excite the field fluctuations.

Table 1 The advantages (+) and disadvantages (−) of the correlation method, the deconvolution method, and the multidimensional deconvolution method

Correlation	Deconvolution	Multidimensional deconvolution
+ exact	+ valid for dissipative systems	+ valid for dissipative systems
+ stable	+ noise spectrum not needed	+ noise spectrum not needed
+ works for two receivers	+ works for two receivers	+ overburden is removed
	+ enhances temporal resolution	+ enhances temporal resolution
− volume sources for dissipative systems	− may be unstable	− needs up/down separation
− needs power spectrum	− correct to first order only	− equation may be ill-posed
		− needs complete coverage

Correlation is a stable process, and one just needs two receivers to extract the fields that propagate between these two receivers. For systems that are not invariant for time-reversal one needs sources throughout the volume to extract the Green's function (Snieder et al. 2007a). Since this condition often is not satisfied in realistic field conditions, this a major drawback for the application to diffusive fields such as pore pressure and low-frequency electromagnetic fields. The absence of noise sources throughout the Earth's volume makes the estimation of attenuation from correlation of recorded seismic noise questionable from a theoretical point of view. Since the Earth is weakly attenuating, the absence of volume source may in practice not be a major problem. It is not clear, though, if under these conditions correlation-based interferometry gives correct estimates of attenuation. Deconvolution interferometry has been used to estimate attenuation (Trampert et al. 1993; Snieder and Şafak 2006), while interferometry based on the cross-coherence, a method originally advocated by Aki (1957), has been used to obtained reasonable models for the attenuation in California (Prieto et al. 2009). As shown in Eq. 3 one must know the power spectrum of the excitation in order to extract the Green's function. For some applications this is not a problem, but in some application this is a restriction that cannot be ignored. As shown by Mehta et al. (2008b), small variations in the characteristics of an airgun source lead in marine seismic applications based on the correlation method to spurious events when those variations are not properly accounted for.

The deconvolution approach also holds for systems that are not invariant for time reversal. Equation 7 gives the perturbed Green's function for the two employed receivers. Note that this expression is solely based on the decomposition of the field in a reference field and a perturbation, but it makes no assumption about the underlying field equation. In the deconvolution approach the spectrum of the excitation need not be known because it does not influence the spectral ratio taken in the deconvolution. This is important in situations where the excitation is unknown, as is the case, for example, in drill-bit seismics (Poletto and Miranda 2004) when the vibrations of the drill-stem have not been recorded. As with the correlation approach one needs just two receivers, unless one employs array techniques, such as frequency-wavenumber filtering, to separate the unperturbed waves from the perturbed waves (Vasconcelos et al. 2008a). The deconvolution corrects for variations in the spectral amplitude of the source, and therefore gives an extracted response with a larger bandwidth than cross-correlation does. This corresponds, in the time domain, to a response with a greater temporal resolution. This difference can clearly be seen by comparing the middle and right panels of Fig. 4. Deconvolution corresponds, in the

frequency domain, to a spectral ratio. This ratio is unstable near notches in the spectrum. Many methods exists to stabilize the deconvolution (Webster 1978); we used the water-level method in our applications. A drawback of the deconvolution is that it does not necessarily produce the Green's function. The extracted response at the reference receiver is a band-limited delta function, the response thus satisfies a clamped boundary condition at that point. In seismic exploration this may introduce spurious reflections, but these spurious reflections leave only a weak imprint on seismic images constructed from multi-offset data (Vasconcelos and Snieder 2008a). On the other hand, in the examples of the analysis of the motion of the Millikan library, the clamped boundary condition could be used the extract the building response under boundary conditions other than those of the physical building. This can be used to unravel the contributions of the mechanical properties of the building from the soil–structure interaction.

The multidimensional deconvolution approach is valid for systems that are invariant for time reversal as well as for those that are not invariant for time-reversal. The spectrum of the excitation needs not be known. In fact, in contrast to the correlation approach, the power spectrum of the excitation may vary between different noise sources, and as with the deconvolution method, this technique leads to a response with a larger temporal resolution than is produced by the cross-correlation. The imprint of the overburden is completely removed from the estimated reflectivity. This is of particular importance in applications where reflections from the free surface or an electromagnetic airwave contaminate measured fields. The method relies on up/down decomposition. This processing step may necessitate the use of arrays or the measurement of additional fields such as pressure and displacement in marine seismology or the measurement of electric and magnetic fields in electromagnetic applications, as well as on estimates of the near-surface impedance. The simultaneous solution of integral equation (9) for a number of sources may be unstable. As with the deconvolution such instability may be suppressed to a certain degree by regularization, or it may require increasing the number of sources used. In order to solve the integral equation, one must have an array of sensors that adequately cover the acquisition surface. This restriction is particularly important when fields are measured only along a line in the acquisition plane.

This overview shows that one has considerable freedom in the choice of the method for extracting the system response from field fluctuations. The overview of merits and drawbacks of Table 1 may aid the reader in choosing the optimal method for a particular application. A property of Green's function extraction that is powerful, but that received little attention, is the freedom that it offers to extract the response of a system that satisfies different boundary conditions from those of the real physical system. This property can be used to alter the contaminating response of the free surface. By comparing the response of the system under different boundary conditions with recorded data it may be possible to estimate the boundary conditions of the physical system. This can potentially be used, for example, in structural engineering to determine the soil–building interaction.

Acknowledgments We thank two anonymous reviewers for their useful corrections and suggestions. This work was supported by the NSF (Grant EAS-0609595), by ExxonMobil Upstream Research Co., and by the GameChanger program of Shell.

References

Aki K (1957) Space and time spectra of stationary stochastic waves with special reference to microtremors. Bull Earthq Res Inst 35:415–456

Amundsen L (2001) Elimination of free-surface related multiples without the need of the source wavelet. Geophysics 66:327–341
Amundsen L, Løseth L, Mittet R, Ellingsrud S, Ursin B (2006) Decomposition of electromagnetic fields into upgoing and downgoing components. Geophysics 71:G211–G223
Bakulin A, Calvert R (2004) Virtual source: new method for imaging and 4D below complex overburden. Expanded abstracts of the 2004 SEG-meeting, pp 2477–2480
Bakulin A, Calvert R (2006) The virtual source method: theory and case study. Geophysics 71:SI139–SI150
Bakulin A, Mateeva A, Mehta K, Jorgensen P, Ferrandis J, Sinha Herhold I, Lopez J (2007) Virtual source applications to imaging and reservoir monitoring. The Leading Edge 26:732–740
Bensen GD, Ritzwoller MH, Barmin MP, Levshin AL, Lin F, Moschetti MP, Shapiro NM, Yang Y (2007) Processing seismic ambient noise data to obtain reliable broad-band surface wave dispersion measurements. Geophys J Int 169:1239–1260
Brenguier F, Campillo M, Hadziioannou C, Shapiro N, Larose E (2008) Postseismic relaxation along the San Andreas Fault at Parkfield from continuous seismological observations. Science 321:1478–1481
Callen HB, Welton TA (1951) Irreversibility and generalized noise. Phys Rev 83:34–40
Campillo M, Paul A (2003) Long-range correlations in the diffuse seismic coda. Science 299:547–549
Chaput JA, Bostock MG (2007) Seismic interferometry using non-volcanic tremor in Cascadia. Geophys Res Lett 34:L07304. doi:10.1029/2007/GL028987
Chávez-Garcia FJ, Luzón F (2005) On the correlation of seismic microtremors. J Geophys Res 110:B11313. doi:10.1029/2005JB003686
Curtis A, Gerstoft P, Sato H, Snieder R, Wapenaar K (2006) Seismic interferometry—turning noise into signal. The Leading Edge 25:1082–1092
Derode A, Larose E, Tanter M, de Rosny J, Tourin A, Campillo M, Fink M (2003a) Recovering the Green's function from far-field correlations in an open scattering medium. J Acoust Soc Am 113:2973–2976
Derode A, Larose E, Campillo M, Fink M (2003b) How to estimate the Green's function for a heterogeneous medium between two passive sensors? Application to acoustic waves. Appl Phys Lett 83:3054–3056
Draganov D, Wapenaar K, Mulder W, Singer J, Verdel A (2007) Retrieval of reflections from seismic background-noise measurements. Geophys Res Lett 34:L04305
Gerstoft P, Fehler MC, Sabra KG (2006) When Katrina hit California. Geophys Res Lett 33:L17308
Griffiths DJ (1999) Introduction to electrodynamics, 3 edn. Prentice Hall, Upper Saddle River
Gutenberg B (1947) Microseisms and weather forecasting. J Meteorol 4:21–28
Hill D, Combee L, Bacon J (2006) Over/under acquisition and data processing: the next quantum leap in seismic technology? First Break 24:81–96
Hornby BE, Yu J (2007) Interferometric imaging of a salt flank using walkaway VSP data. The Leading Edge 26:760–763
Kennett BLN (1979) The suppression of surface multiples on seismic records. Geophys Prosp 27:584–600
Kohler MD, Heaton TH, Bradford SC (2007) Propagating waves in the steel, moment-frame Factor building recorded during earthquakes. Bull Seismol Soc Am 97:1334–1345
Kubo R (1966) The fluctuation–dissipation theorem. Rep Prog Phys 29:255–284
Larose E, Derode A, Campillo M, Fink M (2004) Imaging from one-bit correlations of wideband diffuse wave fields. J Appl Phys 95:8393–8399
Larose E, Montaldo G, Derode A, Campillo M (2006a) Passive imaging of localized reflectors and interfaces in open media. Appl Phys Lett 88:104103
Larose E, Margerin L, Derode A, van Tiggelen B, Campillo M, Shapiro N, Paul A, Stehly L, Tanter M (2006b) Correlation of random wavefields: an interdisciplinary review. Geophysics 71:SI11–SI21
Le Bellac M, Mortessagne F, Batrouni GG (2004) Equilibrium and non-equilibrium statistical thermodynamics. Cambridge University Press, Cambridge
Lobkis OI, Weaver RL (2001) On the emergence of the Green's function in the correlations of a diffuse field. J Acoust Soc Am 110:3011–3017
Longuet-Higgins MS (1950) A theory for the generation of microseisms. Phil Trans R Soc Lond A 243:1–35
Louie JN (2001) Faster, better: shear-wave velocity to 100 meters depth from refraction microtremor analysis. Bull Seismol Soc Am 91:347–364
Malcolm A, Scales J, van Tiggelen BA (2004) Extracting the Green's function from diffuse, equipartitioned waves. Phys Rev E 70:015601
Mehta K, Snieder R, Graizer V (2007a) Downhole receiver function: a case study. Bull Seismol Soc Am 97:1396–1403
Mehta K, Bakulin A, Sheiman J, Calvert R, Snieder R (2007b) Improving the virtual source method by wavefield separation. Geophysics 72:V79–V86
Mehta K, Snieder R, Calvert R, Sheiman J (2008a) Acquisition geometry requirements for generating virtual-source data. The Leading Edge 27:620–629

Mehta K, Sheiman JL, Snieder R, Calvert R (2008b) Strengthening the virtual-source method for time-lapse monitoring. Geophysics 73:S73–S80
Miyazawa M, Snieder R, Venkataraman A (2008) Application of seismic interferometry to extract P and S wave propagation and observation of shear wave splitting from noise data at Cold Lake, Canada. Geophysics 73:D35–D40
Moldoveanu N, Combee L, Egan M, Hamson G, Sydora L, Abriel W (2007) Over/under towed-streamer acquisition: a method to extend seismic bandwidth to both higher and lower frequencies. The Leading Edge 26:41–58
Morse PM, Ingard KU (1968) Theorerical acoustics. McGraw-Hill, New York
Paul A, Campillo M, Margerin L, Larose E, Derode A (2005) Empirical synthesis of time-asymmetrical Green functions from the correlation of coda waves. J Geophys Res 110:B08302. doi:10.1029/2004JB003521
Pharez S, Hendrick N, Tenghemn R (2008) First look at seismic data from a towed dual-sensor streamer. The Leading Edge 27:904–913
Poletto F, Miranda F (2004) Seismic while drilling, fundamentals fo drill-bit seismic for exploration. In: Helbig K, Treitel S (eds) Handbook of geophysical exploration, vol 35. Elsevier, Amsterdam
Poletto F, Malusa M, Miranda F, Tinivella U (2004) Seismic-while-drilling by using dual sensors in drill strings. Geophysics 69:1261–1271
Prieto G, Lawrence JF, Beroza GC (2009) Anelastic earth structure from the coherency of the ambient seismic field. J Geophys Res (submitted)
Rector JW, Marion BP (1991) The use of drill-bit energy as a downhole seismic source. Geophysics 56: 628–634
Rickett JE, Claerbout JF (1999) Acoustic daylight imaging via spectral factorization: helioseismology and reservoir monitoring. The Leading Edge 18:957–960
Rickett JE, Claerbout JF (2000) Calculation of the sun's acoustic impulse response by multidimensional spectral factorization. Sol Phys 192:203–210
Riley DC, Claerbout JF (1976) 2-D multiple reflections. Geophysics 41:592–620
Ritzwoller MH (2009) Ambient noise seismic imaging. In: McGraw Hill yearbook of science and technology 2009. McGraw-Hill, New York
Robinson EA (1999) Seismic inversion and deconvolution. In: Helbig K, Treitel S (eds) Handbook of geophysical exploration, vol 4B. Pergamon, Amsterdam
Roux P, Fink M (2003) Green's function estimation using secondary sources in a shallow water environment. J Acoust Soc Am 113:1406–1416
Roux P, Kuperman WA, NPAL Group (2004) Extracting coherent wave fronts from acoustic ambient noise in the ocean. J Acoust Soc Am 116:1995–2003
Roux P, Sabra KG, Gerstoft P, Kuperman WA (2005) P-waves from cross correlation of seismic noise. Geophys Res Lett 32:L19303. doi:10.1029/2005GL023803
Rytov SM, Kravtsov YuA, Tatarskii VI (1989) Principles of statistical radiophysics, vol 3, elements of random fields. Springer, Berlin
Sabra KG, Roux P, Thode AM, D'Spain GL, Hodgkiss WS (2005a) Using ocean ambient noise for array self-localization and self-synchronization. IEEE J Ocean Eng 30:338–347
Sabra KG, Gerstoft P, Roux P, Kuperman WA, Fehler MC (2005b) Surface wave tomography from microseisms in Southern California. Geophys Res Lett 32:L14311. doi:10.1029/2005GL023155
Sabra KG, Roux P, Gerstoft P, Kuperman WA, Fehler MC (2006) Extracting coherent coda arrivals from cross-correlations of long period seismic waves during the Mount St. Helens 2004 eruption. J Geophys Res 33:L06313. doi:1029.2005GL025563
Sabra KG, Conti S, Roux P, Kuperman WA (2007) Passive in-vivo elastography from skeletal muscle noise. Appl Phys Lett 90:194101
Sabra KG, Srivastava A, di Scalea FL, Bartoli I, Rizzo P, Conti S (2008) Structural health monitoring by extraction of coherent guided waves from diffuse fields. J Acoust Soc Am 123:EL8
Sawazaki K, Sato H, Nakahara H, Nishimura T (2009) Time-lapse changes of seismic velocity in the shallow ground caused by strong ground motion shock of the 2000 Western-Tottori earthquake, Japan, as revealed from coda deconvolution analysis. Bull Seismol Soc Am 99:352–366
Schuster GT, Yu J, Sheng J, Rickett J (2004) Interferometric/daylight seismic imaging. Geophys J Int 157:838–852
Sens-Schönfelder C, Wegler U (2006) Passive image interferometry and seasonal variations at Merapi volcano, Indonesia. Geophys Res Lett 33:L21302. doi:10.1029/2006GL027797
Shapiro NM, Campillo M (2004) Emergence of broadband Rayleigh waves from correlations of the ambient seismic noise. Geophys Res Lett 31:L07614. doi:10.1029/2004GL019491

Shapiro NM, Campillo M, Stehly L, Ritzwoller MH (2005) High-resolution surface-wave tomography from ambient seismic noise. Science 307:1615–1618
Slob E, Draganov D, Wapenaar K (2007) Interferometric electromagnetic Green's functions representations using propagation invariants. Geophys J Int 169:60–80
Snieder R (2004) Extracting the Green's function from the correlation of coda waves: a derivation based on stationary phase. Phys Rev E 69:046610
Snieder R (2006) Retrieving the Green's function of the diffusion equation from the response to a random forcing. Phys Rev E 74:046620
Snieder R (2007) Extracting the Green's function of attenuating heterogeneous acoustic media from uncorrelated waves. J Acoust Soc Am 121:2637–2643
Snieder R, Şafak E (2006) Extracting the building response using seismic interferometry: theory and application to the Millikan library in Pasadena, California. Bull Seismol Soc Am 96:586–598
Snieder R, Sheiman J, Calvert R (2006a) Equivalence of the virtual source method and wavefield deconvolution in seismic interferometry. Phys Rev E 73:066620
Snieder R, Wapenaar K, Larner K (2006b) Spurious multiples in seismic interferometry of primaries. Geophysics 71:SI111–SI124
Snieder R, Wapenaar K, Wegler U (2007a) Unified Green's function retrieval by cross-correlation: connection with energy principles. Phys Rev E 75:036103
Snieder R, Hubbard S, Haney M, Bawden G, Hatchell P, Revil A, Calvert R, Curtis A, Fehler M, Gerstoft P, Hornby B, Landrø M, Lesmes D, Mehta K, Mooney M, Pacheco C, Prejean S, Sato H, Schuster J, Wapenaar K, Wilt M (2007b) Advanced non-invasive geophysical monitoring techniques. Ann Rev Earth Planet Sci 35:653–683
Snieder R, van Wijk K, Haney M, and Calvert R (2008) The cancellation of spurious arrivals in Green's function extraction and the generalized optical theorem. Phys Rev E 78:036606
Stehly L, Campillo M, Shapiro NM (2006) A study of seismic noise from long-range correlation properties. J Geophys Res 111. doi:10.1029/2005JB004237
Stehly L, Campillo M, Froment B, Weaver RL (2008) Reconstructing Green's function by correlation of the coda of the correlation (C3) of ambient seismic noise. J Geophys Res 113:B11306
Tatarskii VP (1987) Example of the description of dissipative processes in terms of reversible dynamic equations and some comments on the fluctuation dissipation theorem. Sov Phys Usp 30:134–152
Thompson D, Snieder R (2006) Seismic anisotropy of a building. The Leading Edge 25:1093
Trampert J, Cara M, Frogneux M (1993) *SH* propagator matrix and Q_s estimates from borehole- and surface-recorded earthquake data. Geophys J Int 112:290–299
Um ES, Alumbaugh DL (2007) On the physics of the marine controlled-source electromagnetic method. Geophysics 72:WA13–WA26
Vasconcelos I, Snieder R (2008a) Interferometry by deconvolution, Part 1—theory for acoustic waves and numerical examples. Geophysics 73:S115–S128
Vasconcelos I, Snieder R (2008b) Interferometry by deconvolution: Part 2—theory for elastic waves and application to drill-bit seismic imaging. Geophysics 73:S129–S141
Vasconcelos I, Snieder R, Hornby B (2008a) Imaging internal multiples from subsalt VSP data—examples of target-oriented interferometry. Geophysics 73:S157–S168
Vasconcelos I, Snieder R, Sava P, Taylor T, Malin P, Chavarria A (2008b) Drill bit noise illuminates the san andreas fault. EOS Trans Am Geophys Union 89(38):349
Verschuur DJ, Berkhout AJ, Wapenaar CPA (1992) Adaptive surface-related multiple elimination. Geophysics 57:1166–1177
Wapenaar K (2004) Retrieving the elastodynamic Green's function of an arbitrary inhomogeneous medium by cross correlation. Phys Rev Lett 93:254301
Wapenaar K, Fokkema J (2006) Green's function representations for seismic interferometry. Geophysics 71(4):SI33–SI46
Wapenaar K, Fokkema J, Dillen M, Scherpenhuijsen P (2000) One-way acoustic reciprocity and its applications in multiple elimination and time-lapse seismics. In: 70th annual SEG meeting, Calgray, expanded abstracts, pp 2377–2380
Wapenaar K, Fokkema J, Snieder R (2005) Retrieving the Green's function by cross-correlation: a comparison of approaches. J Acoust Soc Am 118:2783–2786
Wapenaar K, Slob E, Snieder R (2006) Unified Green's function retrieval by cross-correlation. Phys Rev Lett 97:234301
Wapenaar K, Slob E, Snieder R (2008) Seismic and electromagnetic controlled-source interferometry in dissipative media. Geophys Prosp 56:419–434
Weaver RL (2008) Ward identities and the retrieval of Green's functions in the correlations of a diffuse field. Wave Motion 45:596–604

Weaver RL, Lobkis OI (2001) Ultrasonics without a source: thermal fluctuation correlations at MHz frequencies. Phys Rev Lett 87:134301
Weaver R, Lobkis O (2003) On the emergence of the Green's function in the correlations of a diffuse field: pulse-echo using thermal phonons. Ultrasonics 40:435–439
Weaver RL, Lobkis OI (2005) Fluctuations in diffuse field-field correlations and the emergence of the Green's function in open systems. J Acoust Soc Am 117:3432–3439
Webb SC (1998) Broadband seismology and noise under the ocean. Rev Geophys 36:105–142
Weber J (1956) Fluctuation–dissipation theorem. Phys Rev 101:1620–1626
Webster GM (ed.) (1978) Deconvolution, vol 1 of geophysics reprint series. SEG, Tulsa
Weglein AB, Gasparotto FA, Carvalho PM, Stolt RH (1998) An inverse scattering series method for attenuating multiples in seismic reflection data. Geophysics 62:1975–1989
Wegler U, Sens-Schönfelder C (2007) Fault zone monitoring with passive image interferometry. Geophys J Int 168:1029–1033
van Borselen RG, Fokkema JT, van den Berg PM (1996) Removal of surface-related wave phenomena—the marine case. Geophysics 61:202–210
van Wijk K (2006) On estimating the impulse response between receivers in a controlled ultrasonic experiment. Geophysics 71:SI79–SI84
Yang Y, Ritzwoller MH (2008) Teleseismic surface wave tomography in the western US using the transportable array component of USArray. Geophys Res Lett 5:L04308